2022 Volume 3, Issue 1 : 1 – 16 DOI : 10.48185/jitc.v3i1.489

F-OFDM in a novel form for analyzing 5G networks

Sairoel Amertet*

Department of Mechanical Engineering, Mizan Tepi University, Tepi Ethiopia

Received: 12.05.2022 • Accepted: 07.06.2022 • Published: 30.06.2022 • Final Version: 30.06.2022

Abstract: The need for internet of things (IoT) and machine-to-machine communication (MTC) has been growing rapidly all across the world. To meet the client's needs, many literature reviews were undertaken in several countries. Orthogonal frequency division multiplexing (OFDM), Universal Filtered Multi-Carrier (UFMC), filter-bank multicarrier offset construction amplitude modulation (FBMC-OQAM), generalized frequency division multiplexing (GFDM), and others are candidates for LTE, LTE advance, and 5G, according to the majority of the researchers. However, because it is sensitive to propagation and noise, such as amplitude, with a huge dynamic range, it requires RF power amplifiers with a high peak to average power quantitative relationship; consequently, it is not recommended for LTE, LTE advance, or 5G. As a result, the same concerns were addressed by introducing innovative type filtered orthogonal frequency division multiplexing (F- OFDM), which was the subject of this study. In addition, F-OFDM mathematical models were constructed and simulated in the MATLAB software environment. To validate the proposed innovative F-OFDM, OFDM was compared. For innovative F-OFDM, the simulated result was 0.00083333 bit error rate (BER). Furthermore, the bit error rate (BER) of F-OFDM over OFDM was 89.4 percent, and the peak to average power ratio was 17 percent. The simulation results unmistakably show that the suggested innovative F-OFDM is the greatest fit for LTE, LTE advanced, and 5G contenders.

Keywords: resource block, bit error rate, LTE, LTE advance, 5G, peak to average power

1. Introduction

New data transmission needs have presented an unprecedented difficulty for the cutting-edge cell structure as technology advances[1-2]. Orthogonal frequency division multiplexing (OFDM) has been studied and recognized in broadband wired and wireless standards for over a decade[3-4]. After all, OFDM is currently being employed to meet the tremendous demands of discrete multi-tone transmission (DMT). Asymmetric virtual subscriber line (ADSL) and virtual video broadcasting cable (VVBC) are also available (DVB-C). In addition to the majority of wireless technologies, IEEE 802.11 and IEEE 802.16, long-term evolution superior (LTE-superior), and 5G are all available [5-7]. The intensely spaced orthogonal subcarriers separate the available bandwidth into a collection of slender subcarriers due to the merits of orthogonality [8], [9]. Adaptive modulation methods are also frequently used on subcarrier bands to increase overall bandwidth efficiency. OFDM provides high data rate transmission, reliable multi-route fading, and ease of implementation.[10-12].

Future wireless networks will also be distinguished by a large number of conceivable use cases, such as enhanced cell broadband (eMBB), massive gadget type communications (mMTC), and extremely dependable low latency communications (URLLC). A flexible allocation of available time-frequency property is essential to appropriately support the diversity of use cases[13-15].

^{*} Corresponding Author: sairoel@mtu.edu.et

Despite the fact that OFDM is used in LTE-advanced and 5G networks [16]. The chance filtered-primarily based systems must yet be examined. Filter monetary group multi-service (FBMC) and filtered orthogonal frequency division multiplexing (F-OFDM)[17], [18] are examples of future wireless systems that match the above design requirements. Unlike OFDM, FBMC filters each of the many subcarrier subbands. Both F-OFDM and FBMC have reduced out-of-band (OOB) emissions and better time/frequency localisation houses [19].

Researchers created FBMC and F-OFDM separately[16-20]. And each contains the application of precise signal trends and style assumptions, making it difficult to compare the outcomes. As a result, it's critical to work with a uniform illustration of various waveforms for comparison evaluation. Aside from the standard speech and data benefits of cell phones, 5th generation technology (5G). Gadgets are also predicted to help with traffic, which is expected to be a very common experience in comparison to the normal ones. Device type communication (MTC), for example, employs relatively brief messages and hence the internet of things [21-27].

The employment of adaptive waveforms is a vital step for dealing with looming challenges. Offbeat transmission with a specified cessation is a critical requirement of the waveform configuration in 5G networks. Aim to keep a safe distance from the high overhead of synchronization signals required by large terminals. The cyclic prefix orthogonal frequency division multiplexing technology is used in fourth-generation (4G) structures for modulation and access control (CP-OFDM). Regardless, OFDM is only able to meet the above requirement for explanations. As a result, in eccentric/asynchronous transmission, orthogonality among sub-carriers cannot be stored[28-33]. As a result, unadorned neighbouring channel interference will result from out-of-band (OOB) output. The synchronization overhead, on the other hand, reduces delay and increases electricity consumption. MTC, on the other hand, demands the use of batteries, which must last for a long time. Furthermore, while transmission synchronization is important, time-domain localization properties in 5G waveforms are required to achieve the appropriate latency and message transmission speed. As a result, filtered alerts have been widely seen as long overdue in order to certify the waveform of 5G structures. This is owing to the ability to provide asynchronous transmission using filtered waveforms, which decreases OOB emission, recommends filter-based waveforms, and outperforms OFDM [34-37].

Because of the aforementioned flaws, the second type of filtered-waveforms, sub-band based filtered-waveforms, was developed. This approach will set the filter to cover a sub-band, with each sub-band including many sub-companies eligible for transmission. Because of the wider filter bandwidth, the filter's impulse reaction may be shorter than in the case of sub-service filter operation in many cases. Allow us to provide a brief introduction to the configuration of the fourth technology LTE system in order to encourage a thorough understanding of our claim. LTE (4G) time-area transmission coordinated as periods is currently fashionable. As a result, each period, referred to as the body, lasts 10ms [38-41].

The single individual body is made up of ten sub-frames, each of which takes up the same amount of space in the frame. As a result, one frame contains smaller pieces known as sub-frames, each of which is 1ms long and subdivided similarly into time-slots. Time-slots that is all equal to zero. The CP-OFDM symbols' primary packing containers are 5ms long. As a result, each time slot may include six or seven CP-OFDM symbols, depending on the length of the cyclic prefix, which is determined by the transmission settings. Eventually, the LTE transmission bandwidth capacity will be determined in relation to the total number of subcarriers used for transmission, with each pair of twelve contiguous subcarriers forming a so-called bodily resource block (PRB) or, for convenience,

a useful resource block (RB) [42-48]. The final filtered multi-service (UFMC), which also belongs to the sub-band based entirely filtering group, was another inspiration as a recommended option for 5G. When the UFMC filtering operation is accomplished solely on the transmitter side, only one filter is necessary to maintain the sub-band at the transmitter. The filter out bandwidth could also be increased such that the entire bandwidth of the transmitted sub-bands is filtered at the same time. That example, the simplest one-filter-out on the transmitter may be hired as well. Filtered OFDM is the name for this type of filtered signal (F-OFDM) [49-50].

Every FBMC and F-OFDM is a unique instance of the UFMC, which is worth emphasizing. By reducing the filter length to 1 sub-carrier width, UFMC is reduced to FBMC, and by raising the filter width to the entire authorized bandwidth, UFMC is transformed into F-OFDM, resulting in the general filtered multi-provider decision. Only the F-OFDM improved will be discussed in this work. The remaining sections of this study are as follows: part two is dedicated to the mathematical model of F-OFDM, and section three is dedicated to the results and discussion. Section four contains the conclusion and recommendations.

2. Mathematical models of F-OFDM

We've studied appropriate mathematical models of F-OFDM in this part. A system is usually described by a set of variables and a set of equations that form links between the variables. In addition, we have an F-OFDM transmitter construction. We've created appropriate mathematical models for the F-OFDM transmitter based on the F-OFDM transmitter structure. We've started general OFDM signal equations to get back to F-OFDM acceptable mathematical models. The following is a representation of a general OFDM signal[2-12].

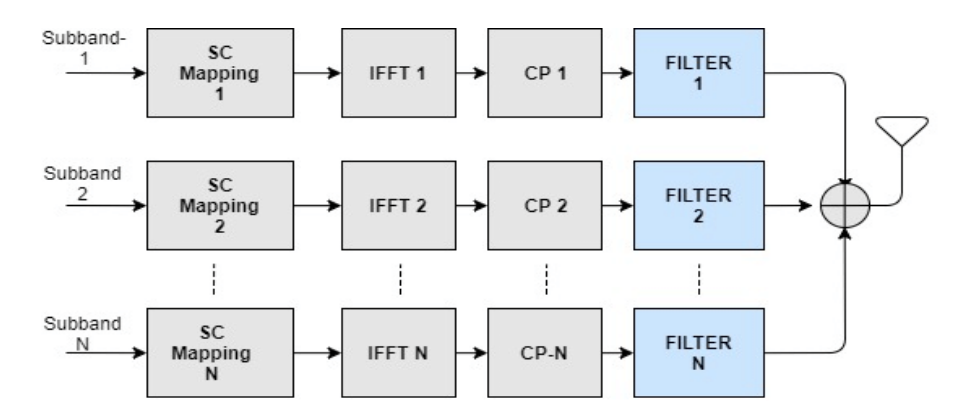


Figure 1. F-OFDM transmitter structure[3]

A block diagram of an F-OFDM transceiver is shown in Figure 1. Bit sequences are converted to BPSK/QAM symbols first. IFFT is then used to map symbols into orthogonal subcarriers, and CP is added after the channel impulse response to avoid inter carrier interference (ICI) and inter Symbol Interference (ISIS) (ISI). It then passes through a pulse shaping filter before broadcasting on a multipath fading channel. F-OFDM is comparable to the Cyclic Prefix OFDM scheme since it has a larger filter length than UFMC and the filter tails extend to surrounding symbols. Implementing this flexible design will provide the desired benefits. To begin, OOBE can be reduced by creating a correct framework for each sub band, which reduces guard band usage. Second, asynchronous transmission can be achieved by using flexible sub-band filter designs. Finally, each user's wants based on their traits can be addressed utilizing optimal numerology.

$$S(t) = \sum_{n = -\infty}^{\infty} S_n(t - nT)$$
 (1)

Where T is the OFDM symbol duration, and sin(t), the nth OFDM symbol of a downlink slot

$$S_n(t) = \sum_{k=0}^{k-1} a_{n,k} \delta(t) \otimes v(t) e^{j2\pi k \Delta f_t}$$

$$= \sum_{k=0}^{k-1} a_{n,k} v(t) e^{j2\pi k \Delta f_t}$$
(2)

Based on Equations (1) and (2), the OFDM signal is derived as:

$$S(t) = \sum_{n = -\infty}^{\infty} S_n(t - nT) = \sum_{n = -\infty}^{\infty} \sum_{k=0}^{k-1} a_{n,k} v(t - nT) e^{j2\pi k \Delta f_t(t - nT)}$$
(3)

After applying the spectrum shaping filter h(t) to the entire sub band described in Equation (1), the F-OFDM signal can be derived as:

$$S(t) = \sum_{n=-\infty}^{\infty} S_n(t - nT) = \sum_{n=-\infty}^{\infty} \left\{ \left[\sum_{k=0}^{k-1} a_{n,k} v(t - nT) e^{j2\pi k \Delta f_t(t - nT)} \right] \otimes h(t - nT) \right\}$$

$$\tag{4}$$

After applying convolution we have been obtained

$$S(t) = \sum_{n=-\infty}^{\infty} \left\{ \left[\sum_{k=0}^{k-1} a_{n,k} v(t-nT) e^{j2\pi k \Delta f_t(t-nT)} \right] \otimes h(t-nT) \right\}$$
 (5)

Unified expression of power spectrum for OFDM, FBMC, and F-OFDM signals equation

$$P_{S}(f) = \frac{|H(f)|^{2} \sigma_{a}^{2} \sum_{k=0}^{k-1} |V(f - k\Delta f)|^{2}}{T}$$
(6)

The PSD of F-OFDM can be described as:

$$P_{S}(f) = |P(f)|^{2} T \sigma^{2} \int_{a}^{a} \sum_{k=0}^{k=1} |\sin c [T(f - k\Delta f)]^{2}$$
(7)

a truncated filter, a window function w(t) applied on an impulse response

$$h(t) = \sin c_{\scriptscriptstyle R}(t)\omega(t) \tag{8}$$

In Equation (8), w(t) has smooth transitions to zero on both ends to avoid abrupt jumps at the beginning and end of the truncated filter, hence avoiding the frequency spill over in the truncated filter, where the bandwidth of the since impulse response is B. Substituting Equation (8) into Equation (7), the PSD of F-OFDM can then be derived as:

$$P_{S}(f) = \left| rect \frac{f}{2B} \otimes w(f) \right|^{2} T \sigma^{2} \int_{k=0}^{k=1} \left| \sin c \left[T \left(f - k \Delta f \right) \right]^{2}$$

$$\tag{9}$$

We have rewritten equation (10)

$$\omega_{H}(t) = \frac{1}{2} [1 + \cos(\frac{2\pi t}{T_{\omega}})] rect(\frac{1}{T_{\omega}})$$

$$= \frac{1}{2} rect(\frac{1}{T_{\omega}}) + \frac{1}{2} \cos(\frac{2\pi t}{T_{\omega}}) rect(\frac{1}{T_{\omega}})$$

$$= \frac{1}{2} rect(\frac{1}{T_{\omega}}) + \frac{1}{4} e^{i(\frac{2\pi t}{T_{\omega}})} rect(\frac{1}{T_{\omega}}) + \frac{1}{4} e^{-j(\frac{2\pi t}{T_{\omega}})} rect(\frac{1}{T_{\omega}})$$

$$(11)$$

Taking a Fourier transform yields:

$$W_{H}(f) = \frac{1}{2} \frac{\sin(\pi T_{\omega} f)}{\pi f} + \frac{1}{4} \frac{\sin(\pi T_{\omega} (f1 - \frac{1}{T_{\omega}}))}{\pi (f - \frac{1}{T_{\omega}})} + \frac{1}{4} \frac{\sin(\pi T_{\omega} (f1 + \frac{1}{T_{\omega}}))}{\pi (f + \frac{1}{T_{\omega}})}$$
(12)

The first term in Equation (12) contributes most to the main lobe, and the second and third terms contribute to doubling the null bandwidth and smoothing the side lobe.

3. Results and discussion

In this section, we compared Orthogonal Frequency Division Multiplexing (OFDM) with Filtered-OFDM (F-OFDM). The merits of the candidate modulation scheme for Fifth Generation (5G) communication systems are highlighted, and filtered-OFDM is validated in LTE and LTE advanced. In F-OFDM, a well-designed filter is applied to the time domain OFDM symbol to boost the out-of-band radiation of the sub-band signal while keeping the OFDM symbols complex-domain Orthogonal.

We might conclude from Figure 2 that the low symbol rate makes the use of a guard period between symbols inexpensive. Additionally, it has the ability to eliminate inter-symbol interference (ISI).

This method also makes it easier to create single-frequency networks (SFNs). Many neighbouring transmitters send a consistent signal at a constant frequency wherever they are. Furthermore, instead of tampering, the signals from numerous distant transmitters are mixed constructively, as would be the case in an extremely old single-carrier system. Nonetheless, the simulation result showed a strong peak-to-average magnitude relationship that was sensitive to frequency offset and, as a result, to Doppler shift[3-9]. As a result, it is not suitable for LTE, enhanced LTE, or 5G. Finally, within the transmission, LTE uses a pre-coded variant of OFDM known as Single Carrier Frequency Division Multiple Access (SC-FDMA)[6-8].

Figure 2. unallocated resource block

This could be to compensate for the disadvantage of classic OFDM, which has a very high Peak to Average Power magnitude relationship (PAPR). High PAPR necessitates expensive and inefficient power amplifiers with a high need for one-dimensionality, which raises the terminal value and drains the battery faster. As shown in figure 4 (a) to (e), the proposed F-OFDM overcomes this disadvantage by grouping along resource blocks in such a way that the necessity for one-dimensionality, and therefore power consumption, inside power electronic equipment is reduced. Coverage and, as a result, cell-edge performance improve with an extra sheet of paper.

Figures 4 (a) to (e) and 5 (a) to (e) show how a band in f-OFDM is divided into multiple sub bands (d). Each band denotes a different sort of data analysis. Another thing to remember is that because each sub-band is made up of multiple subcarriers, the frequency spacing between them varies. We've constructed a really variable structure of sub frame that conveyed the many forms of service information inside an analogous sub frame by combining these sub band flexibility and subcarrier flexibility. Because of the enormous need for 5G, it was almost certain that this form of flexible wave will be used in 5G. Despite the fact that, as shown in Figure 3, (a) to (f), in conventional OFDM, the entire band was made up of one block, and hence the frequency spacing between each subcarrier was the same. Of contrast, the entire band in f-OFDM is made up of numerous sub blocks (sub band). Every sub-band has a completely different subcarrier spacing. Clearly, we have obtained flexibility wave and structure complexity from this study. Furthermore, we learned from this research that f-OFDM stands for Filtered Orthogonal Frequency Division Multiplexing, which is a modification on the basic OFDM technology. Furthermore, it was a very efficient use of spectrum, suppressed Out Of Band Emission, and therefore guard band use could be reduced to a minimum. Furthermore, an optimal subject area has been implemented to meet the needs of bound types of services within each sub-band. Later on, distinct waveforms like as GFDM, FBMC, and UFMC may not be required as optimistically in LTE advanced and 5G, and backward and forward compatibility may be possible. Filtering mostly focused on the victimization sub-band; international synchronization demand was being loosened. As a result, inter-sub-band asynchronous transmission has been made possible[1-4].

The developed filter is applied to the sub-band CP-OFDM signal in F-OFDM. Only a few subcarriers around the sting are affected because the filter's pass band corresponds to the signal's bandwidth. The filter length is allowed to surpass the cyclic prefix length for F-OFD, which is an important concern. Because of the filter's windowing architecture, inter-symbol interference is minimized (with soft truncation). This paper focuses on the essential receive processing for F-OFDM

for one OFDM symbol in the case of an F-OFDM receiver with no channel. After passing through a matching filter, the received signal is sent to a standard CP-OFDM receiver. Prior to the FFT process, it accounts for both the filtering ramp-up and latency. During this study, no fading channel is considered, but noise is injected to the received signal to achieve the desired SNR. At both the transmit and receive ends, F-OFDM adds a filtering stage to the current CP-OFDM processing. The instance simulates a user's full-band allocation, although for an uplink operation, the same approach can be used for several bands (one per user).

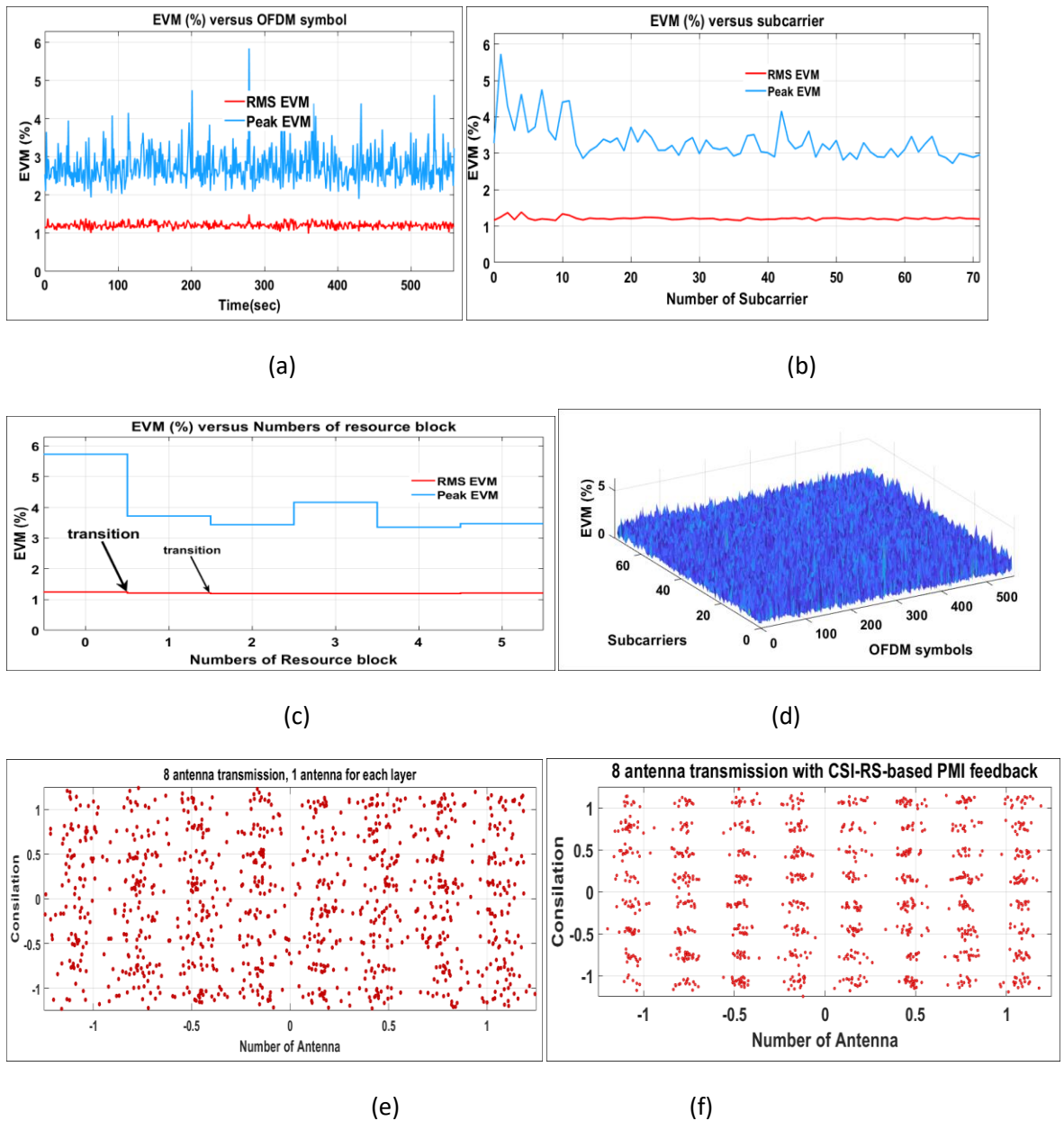


Figure 3. (a) visualization of OFDM interims EVM, (b) Comparison of EVM and number of subcarrier, (c) Comparison of EVM and number of resource blocks, (d) 3D Comparison of EVM and number of subcarrier, OFDM symbols, (e) number of antenna transmission without CSI-RS- based PMI feedback in OFDM, (f) number of antenna transmission with CSI-RSbased PMI feedback in OFDM.

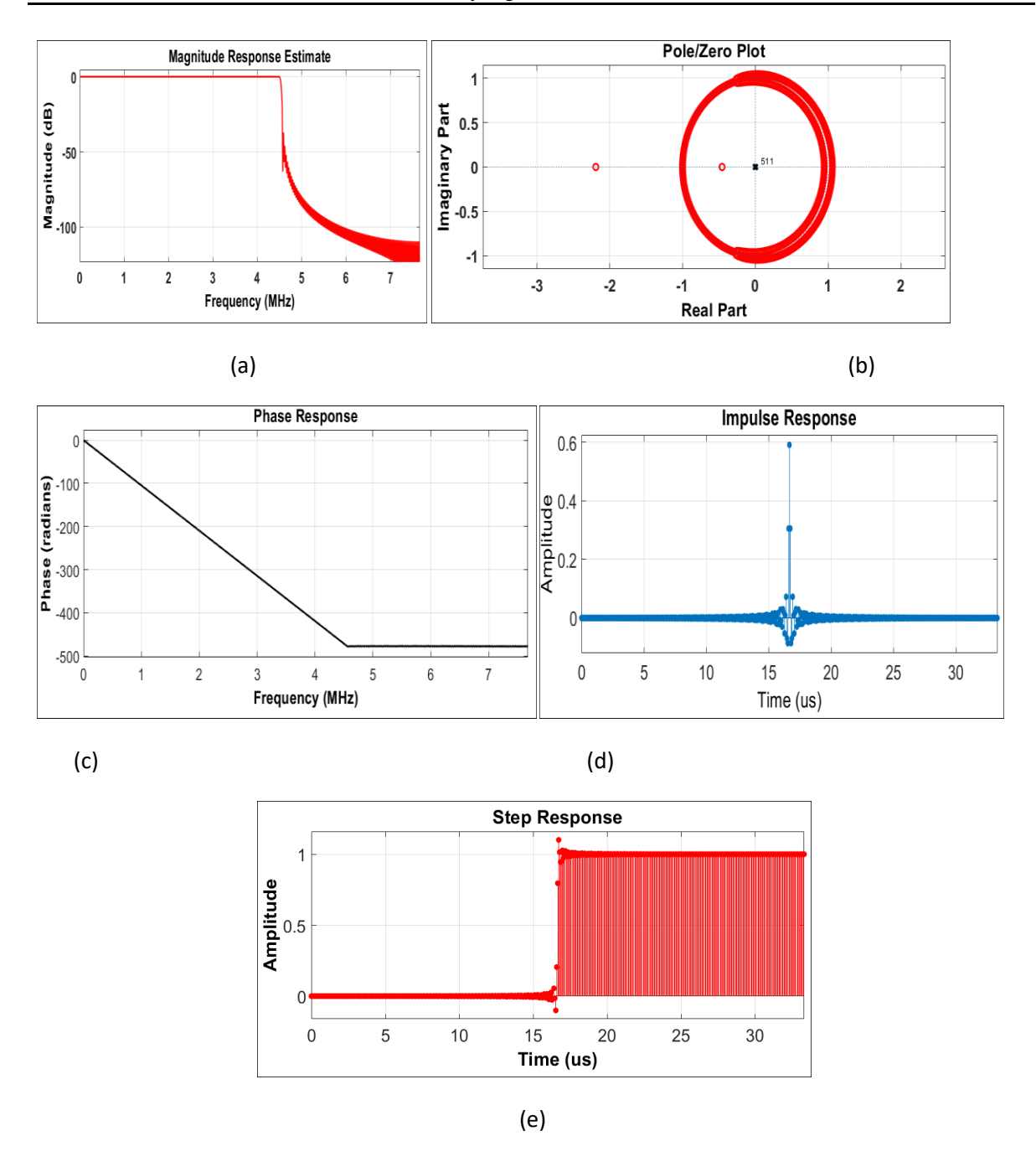


Figure 4. (a) filter visualization magnitude response estimate, (b) pole/zero map, (c) visualization for phase response, (d) impulse response, (e), and step response

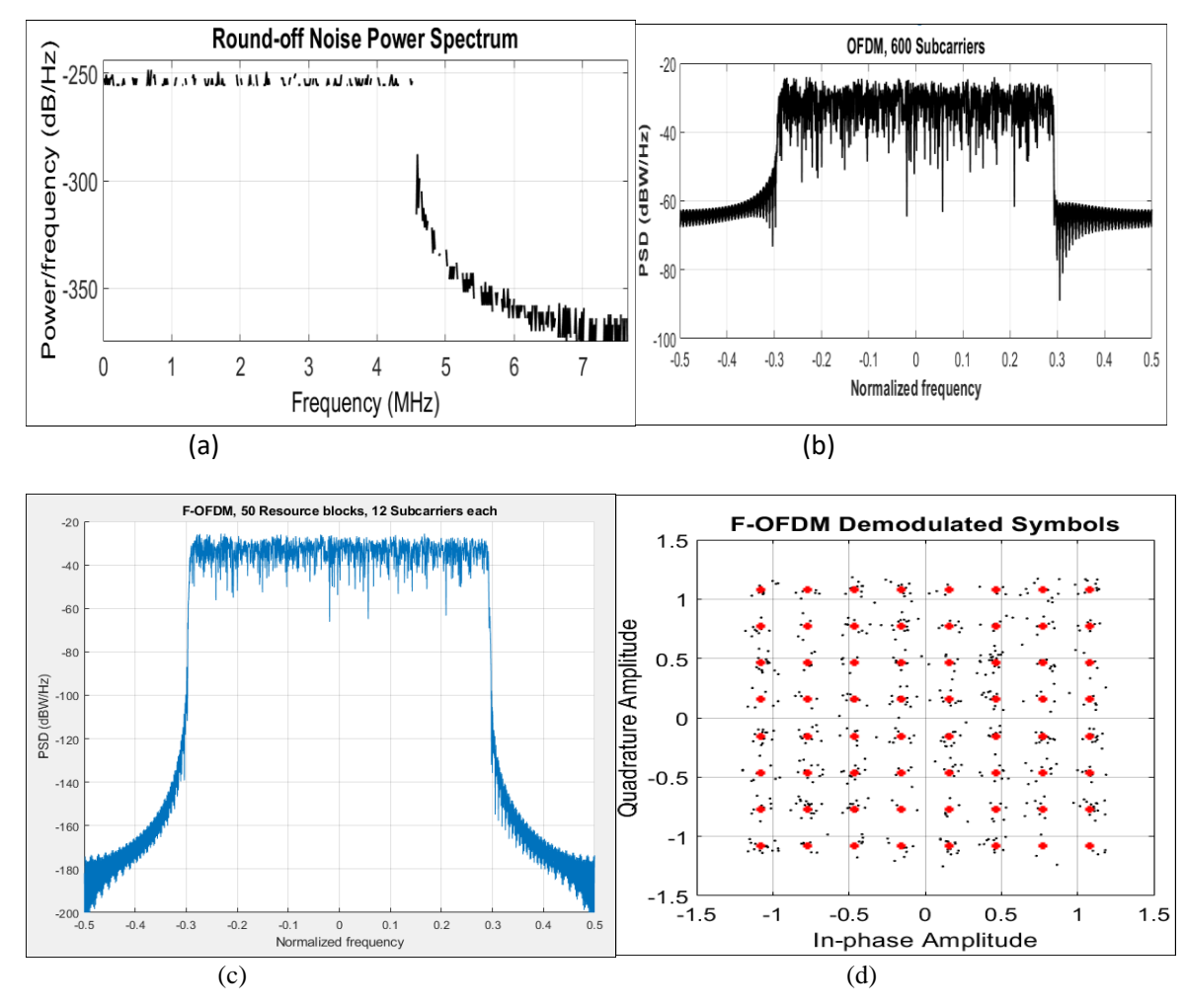


Figure 5. (a) round-off noise power spectrum, (b) OFDM subcarriers, (c) F-OFDM subcarriers, (d) -OFDM demodulated symbols

$$F - OFDM_{Power} = 20\log\left(\frac{F - OFDM_{Peak \text{ to average}}}{OFDM_{Peak \text{ to average}}}\right)$$
(14)

$$F - OFDM \text{ over OFDM}(\%Power) = \frac{\left|OFDM_{power} - F - OFDM_{power}\right|}{OFDM_{power}} *100$$

$$F - OFDM \text{ over OFDM}(\%BER)$$

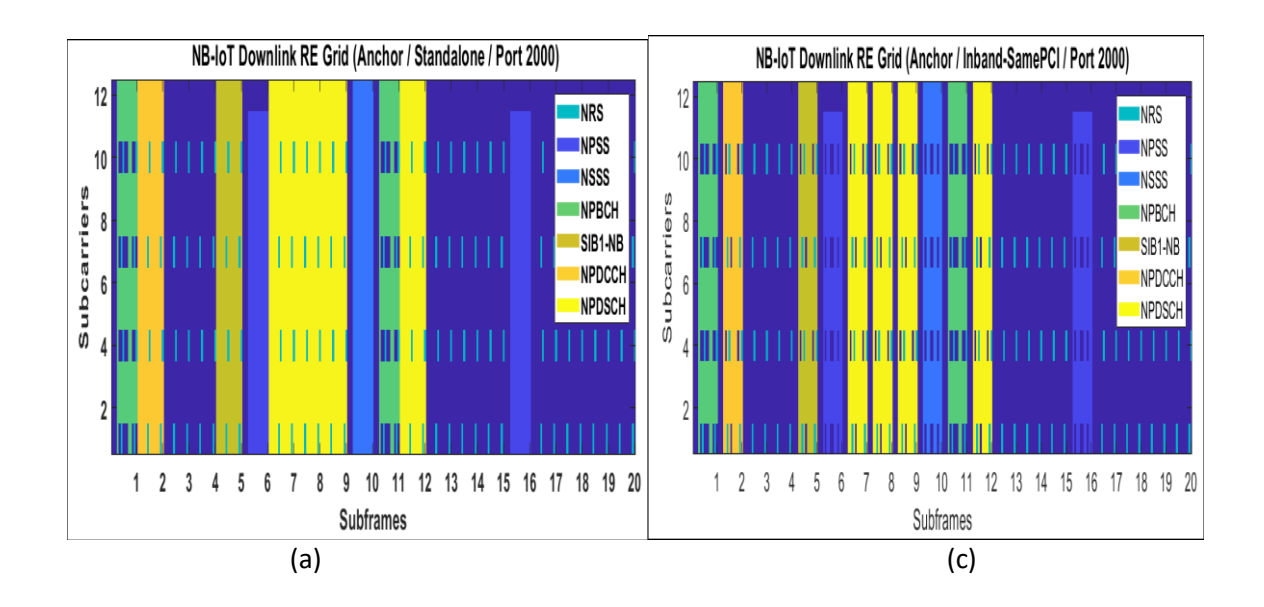
$$\frac{\left|OFDM_{BER} - F - OFDM_{BER}\right|}{OFDM_{BER}} *100$$

Table 1. comparison of F-OFDM over OFDM

Quantity	Peak-to-Average-Power-Ratio (dB), power efficiency	Reception, bit error rate (BER), spectrum	at SNR
	efficiency		
F-OFDM	11.371	0.00083333	18
OFDM	9.721	0.007888	18
F-OFDM	17	89.4	0
over OFDM			
(%)			

Table 2. EVM normalization at average level

Averag	Referenc	Reference	RMS	Peak	Avg	Avg	Avg
e	e phase	constellation	EVM(%	EVM(%	RMS	Peak	MER(dB
reference	offset))	EVM(dB	EVM(dB)
power))	
1	0	Binary	86.3	153.3	-1.3	3.7	1.3
		Phase Shift					
		Keying(BPS					
		K)					
1	$\pi/4$	Quadrature	51.00	88.6	-5.8	-1.1	5.8
		Phase Shift					
		Keying					
		(QPSK)					
1	$\pi/8$	Eight	42.7	87.7	-7.7	-1.1	7.4
		Phase Shift					
		Keying (8-					
		PSK)					
1	0	Quadrature	23.2	43.3	-12.7	-7.3	12.6
		Amplitude					
		Modulation					
		(16-QAM)					
1	0	Quadrature	7.8	20.4	-22.2	-13.8	22.2
		Amplitude					
		Modulation					
		(64-QAM)					
1	0	Quadrature	6.5	11.00	-23.8	-19.2	23.8
		Amplitude					
		Modulation					
		(256-QAM)					



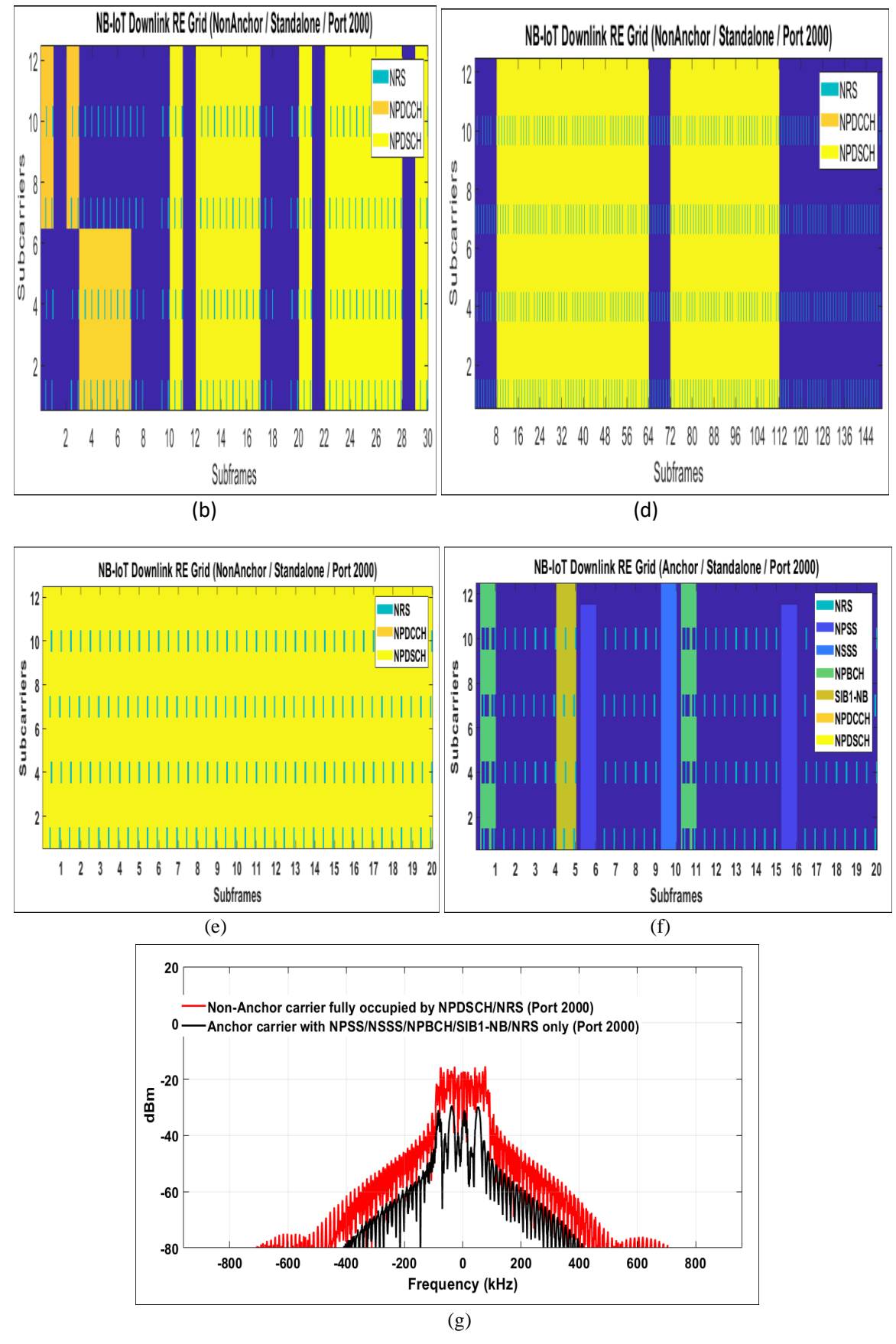


Figure 6. demonstrated that (a) to (g) NB-internet of things (IoT) down link RE grid anchor per standard.

Moreover, figure 6 (b) NB- internet of things (IoT) down link grid anchor per in band-same-PCI. Further figure 6 (c) NB- internet of things (IoT) down link grid non anchor per stand alone, and figure 6 (d) NB- internet of things (IoT) down link grid non anchor per stand alone. Furthermore, figure 6 (e) NB- internet of things (IoT) down link grid non anchor per stand alone. Additionally, figure 6 (f) NB- internet of things (IoT) down link grid anchor per stand alone, and figure (g) depicted that NB- internet of things (IoT) Downlink Waveform generation. In addition to the sub frame allocation described higher up, the generated grids below any justify the RE allocation in a very sub frame, as seen in figures 6(a)-(f). The grid is for two associate degree anchor carrier frames that contain NPSS, NSSS, NRS, NPBCH, SIB1-NB, and NB- internet of things (IoT) downlink sub frames that carry NPDSCH and NPDCCH. As we compared to the standalone and PCI operating modes, in band- grids configurations are the same. This results validate the current work suitable for the 5G telecommunication system[1-10]. Furthermore, the number of NRS ports as well as the narrowband physical cell identification (the parameter fields NBRefP and NNCellID) in structure ngen, Config, will be used to configure out the RE locations. Subsequently, NPSS uses the primary 11 subcarriers, while NSSS uses all 12 subcarriers within a physical resource block [11-13].

The primary 3 OFDM symbols in an exceedingly sub frame aren't used for NPSS/NSSS. On the other hand, NRS isn't transmitted in any sub frame containing NPSS/NSSS as stated in the previous work [4-8]. For this reason the REs of NPSS/NSSS is punctured by the LTE cell-specific reference signal (CRS) only in in-band modes. Furthermore, the amount of CRS ports that affects the puncturing may be configured by parameter field Cell Ref P in structure 5G generation, Configure which is (TS 36.211 10.2.6 and 10.2.7). Due to, NPBCH, the REs are punctured by the NRS and also the CRS using the most number of NRS and CRS antenna ports (2 and 4, respectively), for both operation modes (TS 36.211 10.2.4 [2-4]). This is often because the UE has no knowledge about the amount of used antenna ports and also the operation mode. Based on the NPDSCH operation modes Standalone and Guard band, the REs is punctured by NRS only. On contrast, in-band operation modes, the REs are punctured by both NRS and CRS. For this reason, the primary three OFDM symbols within the sub frame aren't used for NPDSCH carrying SIB1-NB. This leads an NPDSCH is carried by a NB-internet of things (IoT) downlink sub frame.

Control region size could be a parameter field in structure n generation. This configures the LTE control region size for NPDSCH RE allocations that is (TS 36.211 10.2.3, TS 36.213 16.4.1.4, and TS 36.331 6.7.2) as displayed by [1-12] . Therefore, the LTE control region size configures the starting OFDM symbol position during a NB-internet of things (IoT) downlink sub frame carrying NPDSCH and NPDCCH in in-band operation modes. Furthermore, the NRS and CRS puncturing are the identical due to NPDSCH. When the operation mode is in-band, the primary control region size OFDM symbols within the sub frame don't seem to be used for NPDCCH. Same as that for NPDSCH is true that means, control region size is employed to configure the NPDCCH RE allocations (TS 36.211 10.2.3, TS 36.213 16.4.1.4, and TS 36.331 6.7.2). eNodeB configuration parameters fields such as NPBCH, SIB1NPDSCH, NPDCCH, and NPDSCH are created when the NB- (IoT) is used. NPDSCH also configures NPBCH, NPDSCH with SIB1-NB, and NPDCCH. This means that NB-IoT downlink sub frames carry NPDSCH. As a result, NPDSCH and NPDCCH both have a single transport block and a single downlink control information (DCI) message. The parameters of an NPDCCH/NPDSCH are given by a structure, and numerous NPDCCH/NPDSCH area units are expressed as a structure vector, according to earlier work [3-15]. As a result, the planned system has been configured.

4. Conclusion

F-OFDM adds a filtering stage to the current CP-OFDM process at both the transmit and receive ends, as previously stated. The current research used models to allocate a full band to a single user, but a similar strategy will be used for several bands (one per user) in a transmission operation. Furthermore, the current research discusses the fundamental properties of the F-OFDM modulation theme at each of a communication system's transmit and receive endpoints. Then, for the quantity of resource blocks, range of subcarriers per block, filter length, tone offset, and SNR, experiment with completely alternative system parameter settings. F-OFDM and OFDM both use time-domain filtering, but with finer changes in how the filter is intended and used. The length of the filter is forced to be up to the cyclic-prefix length in OFDM, but it will exceed the CP length in F-OFDM. The filter style causes a slight loss in orthogonality (strictly speaking) in F-OFDM, which only impacts the sting subcarriers. As a result, F-OFDM will address the disadvantages of OFDM while maintaining its benefits[1-18]. Because of its overall performance, moderate quality, value, and smoothness, it is used in 5G technology. In comparison to standard OFDM, the F-OFDM requires an additional pair of transmit and receive filters in the transmitter and receiver chains, respectively. CP, like OFDM, can be used to protect signals from ISI in filter-based waveforms like UFMC and F-OFDM. Because full-band filtering can't get rid of any ICI, F-OFDM has it, just as normal OFDM.

References

- [1] X. Yang, S. Yan, X. Li, and F. Li, 'A Unified Spectrum Formulation for OFDM, FBMC, and F-OFDM', Electronics, vol. 9, no. 8, p. 1285, 2020.
- [2] W. Y. Chen, DSL: simulation techniques and standards development for digital subscriber lines. Alpel Publishing, 1997.
- [3] F. A. de Figueiredo, N. F. Aniceto, J. Seki, I. Moerman, and G. Fraidenraich, 'Comparing f-OFDM and OFDM performance for MIMO systems considering a 5G scenario', in 2019 IEEE 2nd 5G World Forum (5GWF), 2019, pp. 532–535.
- [4] X. Zhang, M. Jia, L. Chen, J. Ma, and J. Qiu, 'Filtered-OFDM-enabler for flexible waveform in the 5th generation cellular networks', in 2015 IEEE Global Communications Conference (GLOBECOM), 2015, pp. 1– 6.
- [5] M. Shafi et al., '5G: A tutorial overview of standards, trials, challenges, deployment, and practice', IEEE *J. Sel. Areas Commun.*, vol. 35, no. 6, pp. 1201–1221, 2017.
- [6] A. Zakeri et al., 'Digital transformation via 5G: Deployment plans', in 2020 ITU Kaleidoscope: Industry-*Driven Digital Transformation (ITU K)*, 2020, pp. 1–8.
- [7] J. T. Penttinen, 5G Second Phase Explained: The 3GPP Release 16 Enhancements. John Wiley & Sons, 2021.
- [8] P. Biswas, 'A Simulational Performance of 5G MIMO Systems applying UFMC (Universal Filtered Multicarrier) Study', Turk. J. Comput. Math. Educ. TURCOMAT, vol. 12, no. 2, pp. 3176–3183, 2021.
- [9] I. P. Chochliouros et al., 'Enhanced Mobile Broadband as Enabler for 5G: Actions from the Framework of the 5G-DRIVE Project', in IFIP International Conference on Artificial Intelligence Applications and Innovations, 2019, pp. 31–45.

- [10] S. A. Gbadamosi, G. P. Hancke, and A. M. Abu-Mahfouz, 'Building Upon NB-IoT Networks: A Roadmap Towards 5G New Radio Networks', *IEEE Access*, vol. 8, pp. 188641–188672, 2020.
- [11] M. S. J. Solaija, H. Salman, A. B. Kihero, M. I. Sağlam, and H. Arslan, 'Generalized coordinated multipoint framework for 5G and beyond', *IEEE Access*, 2021.
- [12] W. Zhuang, Q. Ye, F. Lyu, N. Cheng, and J. Ren, 'SDN/NFV-empowered future IoV with enhanced communication, computing, and caching', *Proc. IEEE*, vol. 108, no. 2, pp. 274–291, 2019.
- [13] E. Agrell, T. Eriksson, A. Vardy, and K. Zeger, 'Closest point search in lattices', *IEEE Trans. Inf. Theory*, vol. 48, no. 8, pp. 2201–2214, 2002.
- [14] M. Alshantti, 'Uplink Performance Of Coordinated Multipoint In 5G Cellular Network', *Turk. J. Comput. Math. Educ. TURCOMAT*, vol. 12, no. 11, pp. 1781–1790, 2021.
- [15] Y. G. Li and G. L. Stuber, *Orthogonal frequency division multiplexing for wireless communications*. Springer Science & Business Media, 2006.
- [16] B. Farhang-Boroujeny and H. Moradi, 'OFDM inspired waveforms for 5G', *IEEE Commun. Surv. Tutor.*, vol. 18, no. 4, pp. 2474–2492, 2016.
- [17] R. D. Van Nee and R. Prasad, 'OFDM for wireless multimedia communications', 2000.
- [18] Z. E. Ankarali, B. Peköz, and H. Arslan, 'Flexible radio access beyond 5G: A future projection on waveform, numerology, and frame design principles', *IEEE Access*, vol. 5, pp. 18295–18309, 2017.
- [19] R. Nissel, S. Schwarz, and M. Rupp, 'Filter bank multicarrier modulation schemes for future mobile communications', *IEEE J. Sel. Areas Commun.*, vol. 35, no. 8, pp. 1768–1782, 2017.
- [20] L. Zhang, A. Ijaz, P. Xiao, M. M. Molu, and R. Tafazolli, 'Filtered OFDM systems, algorithms, and performance analysis for 5G and beyond', *IEEE Trans. Commun.*, vol. 66, no. 3, pp. 1205–1218, 2017.
- [21] B. Farhang-Boroujeny, 'OFDM versus filter bank multicarrier', *IEEE Signal Process. Mag.*, vol. 28, no. 3, pp. 92–112, 2011.
- [22] M. Rajabzadeh and H. Steendam, 'Power spectral analysis of UW-OFDM systems', *IEEE Trans. Commun.*, vol. 66, no. 6, pp. 2685–2695, 2017.
- [23] G. Wu, H. Yuan, W. Guo, S. Hu, and S. Li, 'On design of physical random access channel in high-speed railway LTE systems', *Chin. Sci. Bull.*, vol. 59, no. 35, pp. 5042–5050, 2014.
- [24] A. J. Männistö, 'A Study of Hardware Acceleration in System on Chip Designs using Transport Triggered Architecture', Master's Thesis, 2016.
- [25] Farhang-Boroujeny, Behrouz, and ChungHim Yuen. "Cosine modulated and offset QAM filter bank multicarrier techniques: a continuous-time prospect." *EURASIP Journal on Advances in Signal Processing* 2010 (2010): 1-16.
- [26] Van Waterschoot, Toon, Vincent Le Nir, Jonathan Duplicy, and Marc Moonen. "Analytical expressions for the power spectral density of CP-OFDM and ZP-OFDM signals." *IEEE Signal Processing Letters* 17, no. 4 (2010): 371-374.
- [27] Zaidi, Ali, Fredrik Athley, Jonas Medbo, Ulf Gustavsson, Giuseppe Durisi, and Xiaoming Chen. 5G Physical Layer: principles, models and technology components. Academic Press, 2018.

- [28] Mizutani, Keiichi, Takeshi Matsumura, and Hiroshi Harada. "A comprehensive study of universal timedomain windowed OFDM-based LTE downlink system." In 2017 20th International Symposium on Wireless Personal Multimedia Communications (WPMC), pp. 28-34. IEEE, 2017.
- [29] Zhao, Jian. "DFT-based offset-QAM OFDM for optical communications." Optics express 22, no. 1 (2014): 1114-1126.
- [30] Moles-Cases, Vicent, Ali A. Zaidi, Xiaoming Chen, Tobias J. Oechtering, and Robert Baldemair. "A comparison of OFDM, QAM-FBMC, and OQAM-FBMC waveforms subject to phase noise." In 2017 IEEE international conference on communications (ICC), pp. 1-6. IEEE, 2017.
- [31] Luo, Fa-Long, and Charlie Jianzhong Zhang, eds. Signal processing for 5G: algorithms and implementations. John Wiley & Sons, 2016.
- [32] Jayan, Gopika, and Aswathy K. Nair. "Performance analysis of filtered OFDM for 5G." In 2018 International Conference on Wireless Communications, Signal Processing and Networking (WiSPNET), pp. 1-5. IEEE, 2018.
- [33] P de Figueiredo, Felipe A., Dragoslav Stojadinovic, Prasanthi Maddala, Ruben Mennes, Irfan Jabandžić, Xianjun Jiao, and Ingrid Moerman. "Scatter phy: An open source physical layer for the darpa spectrum collaboration challenge." Electronics 8, no. 11 (2019): 1343.
- [34] de Figueiredo, Felipe AP, Ruben Mennes, Irfan Jabandžić, Xianjun Jiao, and Ingrid Moerman. "A baseband wireless spectrum hypervisor for multiplexing concurrent ofdm signals." Sensors 20, no. 4 (2020): 1101.
- [35] Biswas, Preesat. "A Simulational Performance of 5G MIMO Systems applying UFMC (Universal Filtered Multicarrier) Study." Turkish Journal of Computer and Mathematics Education (TURCOMAT) 12, no. 2 (2021): 3176-3183.
- [36] de Figueiredo, Felipe AP, Claudio F. Dias, Eduardo R. de Lima, and Gustavo Fraidenraich. "Performance analysis of large-scale MU-MIMO with a simple and effective channel estimator." In 2019 IEEE Latin-American Conference on Communications (LATINCOM), pp. 1-6. IEEE, 2019.
- [37] De Figueiredo, Felipe AP, Fabbryccio ACM Cardoso, Ingrid Moerman, and Gustavo Fraidenraich. "On the application of massive MIMO systems to machine type communications." IEEE access 7 (2018): 2589-2611.
- [38] Zhang, Xi, Ming Jia, Lei Chen, Jianglei Ma, and Jing Qiu. "Filtered-OFDM-enabler for flexible waveform in the 5th generation cellular networks." In 2015 IEEE Global Communications Conference (GLOBECOM), pp. 1-6. IEEE, 2015.
- [39] Proakis, John G., Masoud Salehi, Ning Zhou, and Xiaofeng Li. Communication systems engineering. Vol. 2. New Jersey: Prentice Hall, 1994.
- [40] Kobayashi, Ricardo Tadashi, and Taufik Abrão. "FBMC prototype filter design via convex optimization." IEEE Transactions on Vehicular Technology 68, no. 1 (2018): 393-404.
- [41] Tadashi Kobayashi, Ricardo, and Taufik Abrao. "FBMC Prototype Filter Design via Convex Optimization." arXiv e-prints (2018): arXiv-1810.
- [42] Le Floch, Bernard, Michel Alard, and Claude Berrou. "Coded orthogonal frequency division multiplex [TV broadcasting]." Proceedings of the IEEE 83, no. 6 (1995): 982-996.

- [43] Mirabbasi, Shahriar, and Ken Martin. "Overlapped complex-modulated transmultiplexer filters with simplified design and superior stopbands." *IEEE Transactions on Circuits and Systems II: Analog and Digital Signal Processing* 50, no. 8 (2003): 456-469.
- [44] Moore, Ian C., and Michael Cada. "Prolate spheroidal wave functions, an introduction to the Slepian series and its properties." *Applied and Computational Harmonic Analysis* 16, no. 3 (2004): 208-230.
- [45] Haas, Ralf, and Jean-Claude Belfiore. "A time-frequency well-localized pulse for multiple carrier transmission." *Wireless personal communications* 5, no. 1 (1997): 1-18.
- [46] Prakash, J. Arun, and G. Ramachandra Reddy. "Efficient prototype filter design for Filter Bank Multicarrier (FBMC) System based on Ambiguity function analysis of Hermite polynomials." In 2013 International Multi-Conference on Automation, Computing, Communication, Control and Compressed Sensing (iMac4s), pp. 580-585. IEEE, 2013.
- [47] Aminjavaheri, Amir, Arman Farhang, Linda E. Doyle, and Behrouz Farhang-Boroujeny. "Prototype filter design for FBMC in massive MIMO channels." In 2017 IEEE International Conference on Communications (ICC), pp. 1-6. IEEE, 2017.
- [48] Bellanger, Maurice, D. Le Ruyet, D. Roviras, M. Terré, J. Nossek, L. Baltar, Q. Bai, D. Waldhauser, M. Renfors, and T. Ihalainen. "FBMC physical layer: a primer." *Phydyas* 25, no. 4 (2010): 7-10.
- [49] Lopes Ferreira, Mário, and João Canas Ferreira. "An FPGA-oriented baseband modulator architecture for 4g/5g communication scenarios." *Electronics* 8, no. 1 (2019): 2.
- [50] Abdoli, Javad, Ming Jia, and Jianglei Ma. "Filtered OFDM: A new waveform for future wireless systems." In 2015 IEEE 16th International Workshop on Signal Processing Advances in Wireless Communications (SPAWC), pp. 66-70. IEEE, 2015.

Appendix

3GPP TS 36.211 "Physical channels and modulation"

3GPP TS 36.212 "Multiplexing and channel coding"

3GPP TS 36.213 "Physical layer procedures"

3GPP TS 36.321 "Medium Access Control (MAC); Protocol specification"

3GPP TS 36.331 "Radio Resource Control (RRC); Protocol specification"

3GPP TS 36.300 "Overall description; Stage 2"

3GPP TS 36.101 "User Equipment (UE) radio transmission and reception"

3GPP TS 36.141 "Base Station (BS) conformance testing"